



ERNEST ORLANDO LAWRENCE BERKELEY NATIONAL LABORATORY

Optimization of Signal Extraction and Front-End Design in a Fast, Multigap Ionization Chamber

P.S. Datte, P.F. Manfredi, J.E. Millaud, M. Placidi,
L. Ratti, V. Speziali, G. Traversi, and W.C. Turner

**Accelerator and Fusion
Research Division**

November 2001

Presented at the
*IEEE Nuclear Science
Symposium (NSS 2001)*,
San Diego, CA,
November 5-9, 2001,
and to be published in
the Proceedings

DISCLAIMER

This document was prepared as an account of work sponsored by the United States Government. While this document is believed to contain correct information, neither the United States Government nor any agency thereof, nor The Regents of the University of California, nor any of their employees, makes any warranty, express or implied, or assumes any legal responsibility for the accuracy, completeness, or usefulness of any information, apparatus, product, or process disclosed, or represents that its use would not infringe privately owned rights. Reference herein to any specific commercial product, process, or service by its trade name, trademark, manufacturer, or otherwise, does not necessarily constitute or imply its endorsement, recommendation, or favoring by the United States Government or any agency thereof, or The Regents of the University of California. The views and opinions of authors expressed herein do not necessarily state or reflect those of the United States Government or any agency thereof, or The Regents of the University of California.

Ernest Orlando Lawrence Berkeley National Laboratory
is an equal opportunity employer.

Optimization of Signal Extraction and Front-End Design in a Fast, Multigap Ionization Chamber

P.S. Datte,¹ P.F. Manfredi,^{1,2,3} J.E. Millaud,⁴ M. Placidi,^{2,3}
L. Ratti,^{2,3} V. Speziali,^{2,3} G. Traversi,^{2,3} and W.C. Turner⁴

¹Accelerator and Fusion Research Division
Ernest Orlando Lawrence Berkeley National Laboratory
University of California
Berkeley, California 94720

²Università di Pavia
Dipartimento di Electronica
Via Ferrata 1
27100 Pavia, Italy

³INFN
Sezione di Pavia
Via Bassi 6
27100 Pavia, Italy

⁴CERN
Geneva, Switzerland

November 2001

Optimization of signal extraction and front-end design in a fast, multigap ionization chamber

P.S. Datte^{1,*}, P.F. Manfredi^{1,2,3}, J.E. Millaud¹, M. Placidi⁴, L. Ratti^{2,3}, V. Speziali^{2,3}, G. Traversi^{2,3}, W.C. Turner¹

¹ Lawrence Berkeley National Laboratory, 1 Cyclotron Rd, Berkeley CA 94720, USA

² Università di Pavia, Dipartimento di Elettronica, Via Ferrata 1, 27100 Pavia, Italy

³ INFN, Sezione di Pavia, Via Bassi 6, 27100 Pavia, Italy

⁴ CERN, Geneva, Switzerland

Abstract—This paper discusses the criteria that have been adopted to optimize the signal processing in a shower detector to be employed as LHC beam luminosity monitor. The original aspect of this instrument is its ability to operate on a bunch-by-bunch basis. This means that it must perform accurate charge measurements at a repetition rate of 40 MHz. The detector must withstand an integrated dose of 100 Grad, that is, two to three orders of magnitude beyond those expected in the experiments. To meet the above requirements, an ionization chamber consisting of several gaps of thickness 0.5 mm, filled with a gas that is expected to be radiation resistant, has been designed. Crucial in the development of the system is the signal processing, as the electronics noise may set the dominant limitation to the accuracy of the measurement. This is related to two aspects. One is the short time available for the charge measurement. The second one is the presence of a few meter cable between the detector and the preamplifier, as this must be located out of the region of highest radiation field. Therefore the optimization of the signal-to-noise ratio requires that the best configuration of the chamber gaps be determined under the constraint of the presence of a cable of non negligible length between detector and preamplifier. The remote placement of the amplifying electronics will require that the front-end electronics be radiation hard although to a lesser extent than the detector.

I. INTRODUCTION

A high flux of forward neutral particles is produced when the 7 TeV proton beams of the LHC are in collision at the high luminosity interaction points. Some of the neutrals that originate from the proton interaction propagate inside the beam pipe until reaching the cryogenic separation dipole magnets. Absorbers are placed in front of these magnets to prevent quenching by the energy deposition from these neutral particles. As the neutral particles enter the absorber a shower (hadronic and electromagnetic) is created that is directly proportional to the number of neutral particles and hence to the luminosity. Placing a detector to measure the shower intensity at the shower maximum provides a direct measurement of the luminosity as well as other operational information to aid the collision optimization. The shower detector is a multigap ionization chamber filled with a mixture of inorganic gases. This unique approach requires that the detection system be able to perform accurate charge measurement on the bunch-by-bunch basis of 40 MHz. The detector will be exposed to an

extremely high radiation dose, up to an integrated value of more than 100 Grad over the 10 operational years of the LHC. The requirement of such an advanced radiation hardness phases out mixture of gases containing organic molecules ([4], [5]). However, to attain the 40 MHz repetition rate in the charge measurement, the detector signal must be short enough to be compatible with the constraint that the shaped analog signal must return to zero within the 25 ns interbunch period of LHC. This means that the detector current pulse must have a duration comparable or shorter than 25 ns to keep the ballistic deficiency to an acceptable value. The requirement of having a comparatively short signal from the chamber, that is, sufficiently high electron drift velocity without adding organic molecules to the filling gas has been solved by adopting a mixture of inorganic gases (Ar+2%N₂). Such a mixture was proven to feature an electron drift velocity of 3.2 cm/ μ s at an electric field-to-pressure ratio of 1200 V/(cm-atm). The sensitive volume of the chamber is divided into thin gaps 0.5 mm each, so that the signal induced on each gap by a MIP crossing it is a triangular pulse of 16 ns basewidth. In order to assure a sufficient volume of detecting material the chamber consists of a total of 60 gaps.

A charge measurement of sufficient accuracy at a repetition rate of 40 MHz is not an easy task and special criteria for signal extraction and front-end design are required. No active device would stand the radiation field in the detector region, so it was decided to locate the front-end amplifier a few meters away from the region of highest intensity. A special radiation hard cable is employed to transfer the chamber signal to the preamplifier. The preamplifier is based on a fast charge sensitive loop which fulfills also the function of providing a low noise termination to the rad-hard cable. This paper describes the way the signal extraction from the chamber and the signal processing were optimized in order to achieve the best signal-to-noise ratio. The optimization process has involved the configuration of the chamber gaps and the design of the analog processing electronics.

II. SIGNAL EXTRACTION AND PROCESSING

The accuracy in the measurement of the charge produced in the detector by an individual shower is limited by the electronic noise. The problem of optimizing the signal-to-noise ratio in the present case can be formulated in the

* Corresponding author

following way. The starting point is a detector of $m \times n$ gaps where m and n are two integers. When one or more MIPs cross the chamber it may be assumed, by neglecting the Landau fluctuations, that the same amount of charge is induced in each gap. The first step to be taken is the choice of the active front-end device. The bipolar transistor is considered the most suitable solution in this case for two reasons:

1. it is sufficiently radiation hard to stand the dose present in the location where it will be installed;
2. the cold resistance presented at its input port by a charge sensitive preamplifier employing a bipolar transistor as a front-end device is predictable and stable in temperature to a satisfactory extent.

Consider the case where the detector current is a δ -impulse of charge Q . The square of the signal-to-noise ratio η_s^2 for the bipolar transistor charge sensitive preamplifier followed by a shaper of peaking time t_p is:

$$\eta_s^2 = \frac{Q^2}{\frac{2(kT)^2}{qI_C} \cdot A_1 C_D \cdot \frac{1}{t_p} + \frac{2qI_C}{\beta} A_3 t_p} \quad (1)$$

In equation (1) k is the Boltzmann constant, T is the absolute temperature, q is the elementary charge, I_C is the collector current of the bipolar transistor, A_1 and A_3 are the coefficients of the shaper, C_D is the detector capacitance and β is the current gain of the bipolar transistor. The preamplifier input capacitance C_i has been neglected on account of the fact that the type of transistor employed here has a very high transition frequency. The signal-to-noise ratio has a maximum at

$$I_C t_p = \frac{kT}{q} \cdot \frac{A_1}{A_3} \cdot \beta C_D^2 \quad (2)$$

Its value is

$$\eta_{s,opt}^2 = \frac{Q^2}{4kT C_D \cdot \sqrt{\frac{A_1 A_3}{\beta}}} \quad (3)$$

The property of the bipolar transistor that the variable determining η_{opt} is the product $I_C \cdot t_p$ is of crucial importance in this application. t_p is, indeed, constrained by the counting rate requirements of the system. At a fixed t_p the operating point of the bipolar transistor that guarantees the optimum η is simply fixed by acting on its standing collector current.

The requirement that the system be able to perform charge measurement at 40 MHz implies that the analog processing channel must respond to a delta impulse simulating the chamber current with a weighting function of about 5 ns base width. This corresponds to a peaking time t_p of a few nanoseconds. This is a conservative estimate, which makes allowance for possible fluctuations in the drift velocity of the electrons in the gas.

Having chosen the front-end device the next step is the choice of the gap configuration. It will be shown in the appendix that in a detector consisting of a total number of gaps $n \times m$, with the same charge induced in each gap,

the signal-to-noise ratio is independent of the way the gaps are connected, provided that the square of the signal to noise ratio of the analog processor be related to the detector capacitance and to the charge to be measured by the relationship:

$$\eta^2 = \zeta \cdot \frac{Q^2}{C_D} \quad (4)$$

where ζ is a constant which depends on the weighting function of the shaper and on the noise associated with the front-end element. Comparing (4) with (3) it can be concluded that the bipolar transistor in its optimum operating point satisfies the condition under which the signal-to-noise ratio is independent of the gap configuration. In other words, the signal-to-noise ratio will be the same if the $n \times m$ gaps are connected in series or in parallel or if m branches, each consisting of the series connection of n gaps, are connected in parallel. Such an independence of the signal-to-noise ratio from the gap configuration has been utilized as a degree of freedom to determine the detector capacitance on the basis of the following considerations. Remembering that a cable is inserted between detector and preamplifier, the condition which governs the choice of the gap configuration is the one which leads to an equivalent capacitance such that the cable degrades the signal-to-noise ratio to the least possible extent. In the actual case, the characteristic impedance of the cable, which determines the detector time constant $R_0 C_D$ is 50 Ω . The cable delay is approximately 15 ns. Based on the analysis carried out in reference [6] the value of the equivalent detector capacitance has been chosen to be about 50 pF. With this capacitance value and the other parameters of the system, the degradation in signal-to-noise ratio due to the introduction of the cable would be about 20 %. The configuration of the gaps is accordingly defined taking into account that each gap has a capacitance of about 28 pF. Once C_D and t_p are fixed, the optimum current I_C in the bipolar transistor can be determined from equation (2). Taking into account the ballistic deficit due to the finite width of the actual detector current, the value of η_{opt}^2 can be written as

$$\eta_{opt}^2 = \frac{\sigma^2 m n Q_{gap}^2}{4kT C_{gap} \cdot \sqrt{\frac{A_1 A_3}{\beta}}} \quad (5)$$

where σ is the ballistic deficiency.

III. DESCRIPTION OF THE ANALOG PROCESSOR

The analog processor consists of the charge sensitive preamplifier which provides the cold resistance termination to the rad hard cable, followed by a pole-zero cancellation network, two amplification stages, a baseline restorer and an output buffer (figure 1). The charge sensitive loop employs at the input four transistors in parallel (Q_1 through Q_4) to reduce the thermal noise contribution due to the diffused base resistances $r_{BB'}$ [7].

The transistors are BFP540 and were chosen on the basis of their low $r_{BB'}$, 2.7 Ω for each transistor, resulting in

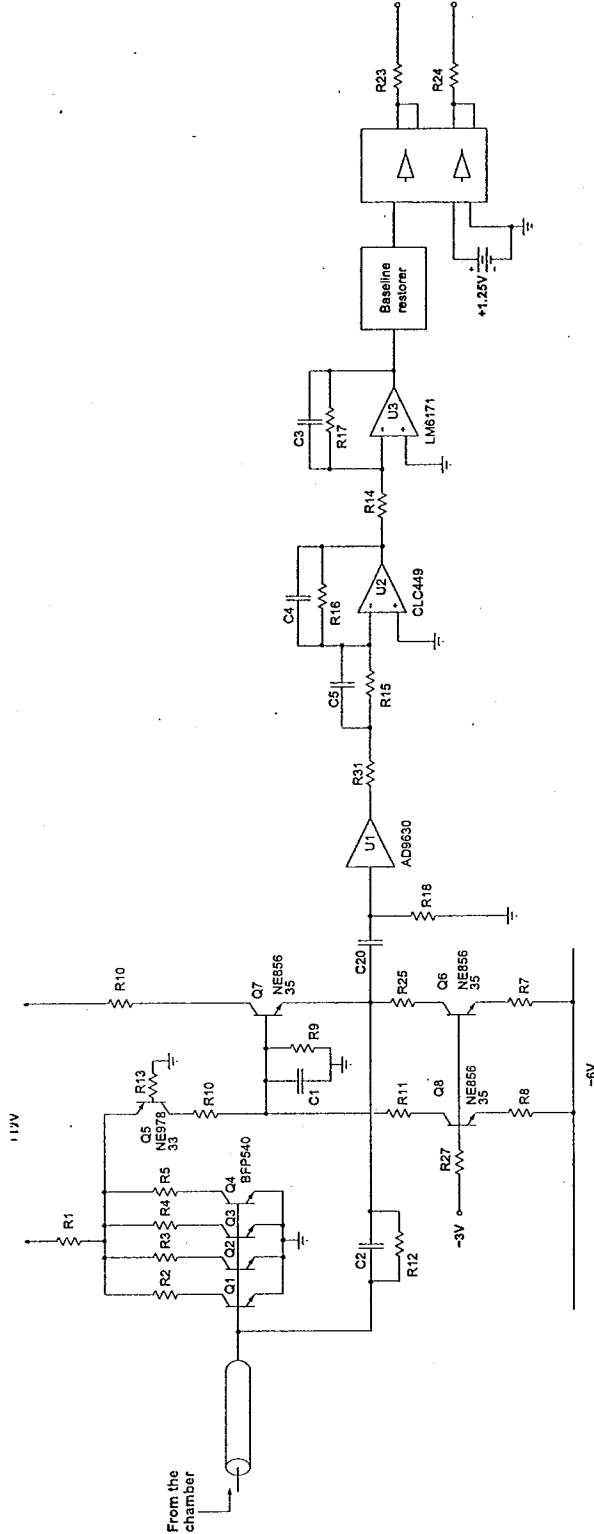


Fig. 1. Schematic of the analog processor associated with the multi-gap ionization chamber.

a spreading resistance of about $1\ \Omega$ for the parallel combination of four of them. They also feature a high transition frequency at currents in the milliamperage range and a high β . They operate at a $1.25\ \text{mA}$ standing current thereby featuring a total transconductance $g_{mT} = 200\ \text{mS}$. The C_1/C_2 ratio is such that $\frac{1}{g_{mT}} \cdot \frac{C_1}{C_2} = 50\ \Omega$, equal to the characteristic impedance of the rad-hard cable. The very effective cable matching feature of the charge sensitive loop is demonstrated by figures 2 and 3 a), b) and c). The magnitude of the impedance seen at the input port of the charge sensitive loop of figure 1 is shown as a function of frequency in figure 2. In the frequency range of interest, from $5\ \text{MHz}$ to several tens of MHz , the behavior of the input impedance is very close to that of a pure $50\ \Omega$ resistor. An inductive term appears at higher frequencies and is to be attributed to the secondary pole in the preamplifier.

The waveforms of figure 3 a), b) and c) are the responses of the entire analog channel to a triangular current signal of $10\ \text{ns}$ basewidth injected across a $50\ \text{pF}$ capacitor simulating the chamber. The waveform in figure 3 a) is relevant to the case of absence of cable. The waveforms in figures 3 b) and c) refer to the case respectively of three and six meter cables inserted between the detector and the preamplifier. As shown in figures 3 a), b) and c) the reflection are barely noticeable in the displayed amplitude scale.

The output from the charge sensitive loop is AC coupled to the buffer U_1 , whose output signal goes to the circuit designed around the operational amplifier U_2 . This circuit compensates the pole $C_2 R_{12}$ in the charge-sensitive loop with the zero determined by $C_5 R_{15}$ and performs the first integration of time constant $C_4 R_{16}$. The circuit designed around the operational amplifier U_3 introduces the second integration with time constant $C_3 R_{17}$. The baseline restorer between U_3 and the final buffer is designed to have a mild restoration rate with the purpose of acting on the average baseline shift at high rates without introducing too much of a degradation on the signal to noise ratio.

The noise behavior of the analog channel is described in figure 4 where the equivalent noise charge ENC is plotted as a function of the detector capacitance in the case of

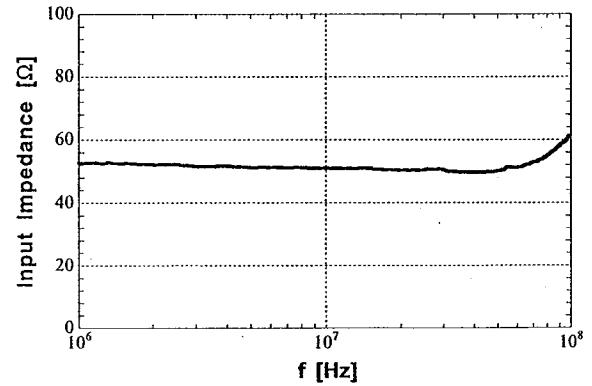


Fig. 2. Magnitude of the impedance seen at the input of the charge sensitive loop of figure 1 as a function of frequency.

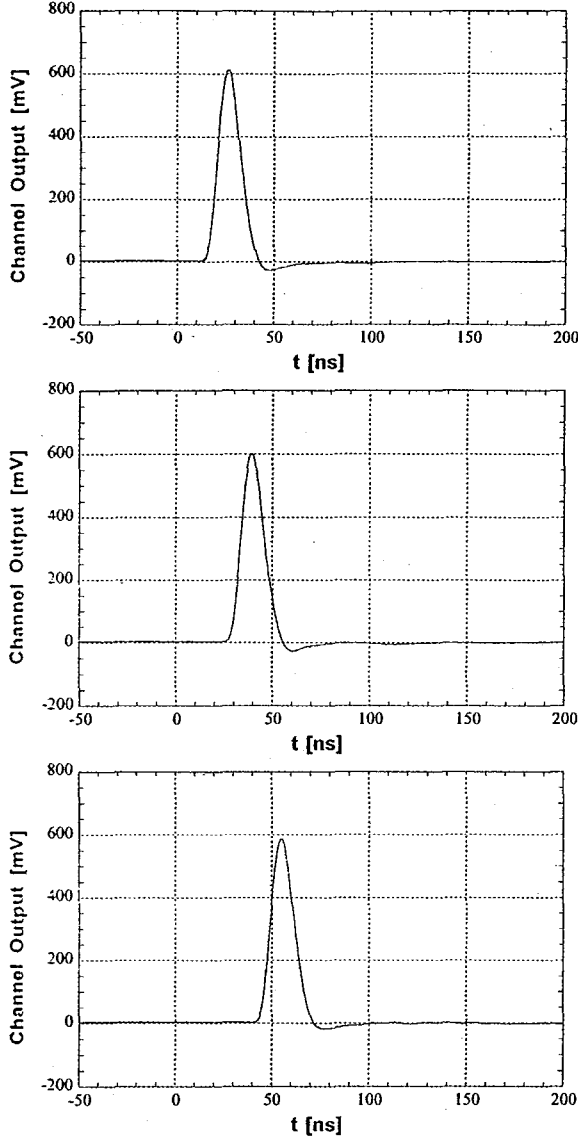


Fig. 3. Response of the analog processor to a 10 ns basewidth triangular signal simulating the detector current: a) direct connection between detector and preamplifier; b) 3 m long radiation hard cable inserted between detector and preamplifier; c) 6 m long radiation hard cable inserted between detector and preamplifier.

direct connection between detector and preamplifier and in the case of a 3 m rad-hard cable inserted between them. The plot shows that the cable degradation is about 20 % which is fully consistent with the theoretical prediction. It might be interesting to point out that if the same cable were not terminated at the receiving end, therefore behaving as a capacitance, the equivalent noise charge in presence of the cable would be approximately 6500 electrons rms. This highlights once again the advantage of using a cold resistance as a matching termination.

The ability of the system to perform charge measure-

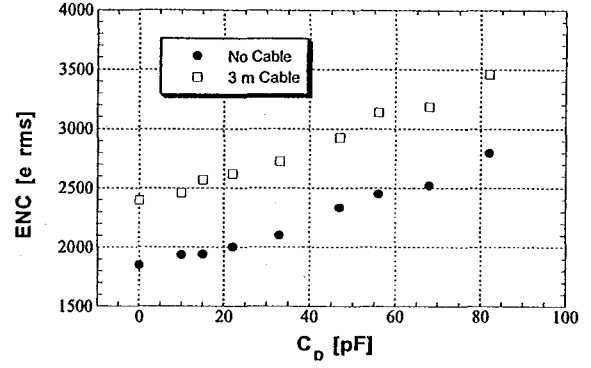


Fig. 4. Equivalent noise charge as a function of the equivalent detector capacitance.

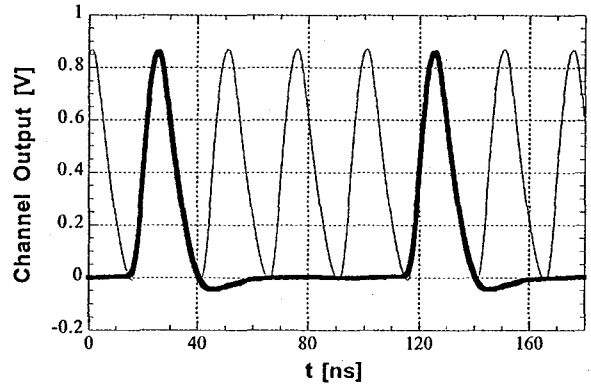


Fig. 5. Response of the analog processor to a 40 MHz sequence of current pulses simulating the bunch-by-bunch charge injection at LHC. The two signals in heavier line are obtained by injecting the same charge at a four times smaller repetition rate.

ments at a repetition rate of 40 MHz is shown in figure 5, which compares the channel output at a charge injection rate of 10 MHz with the output at an injection rate of 40 MHz. The variation in amplitude and shape of the channel output in the two situations is negligible.

IV. ACHIEVABLE SIGNAL-TO-NOISE RATIO

This section is based on the analysis of the signal-to-noise ratio available with the actual detection system and for this purpose reference will be made to equation (5), which is repeated here:

$$\eta_{opt}^2 = \frac{\sigma^2 m n Q_{gap}^2}{4kT C_{gap} \cdot \sqrt{\frac{A_1 A_2}{\beta}}}$$

The multigap chamber to which the processor described in the previous section is to be associated, consists of a total of $n \times m = 60$ square gaps of 4 cm side and 0.5 mm thickness. The capacitance C_{gap} of each gap is 28 pF. The chamber will be installed inside the absorbers that shield the superconducting magnets from the forward particles emerging

from pp interactions and positioned in correspondence of the maximum of the showers developing in the absorbers. In this section it will be shown that the developed system is able to detect a single pp interaction. The shower determined by a single pp interaction consists on average of 380 MIPs, each of them delivering about 5 electrons in the 0.5 mm gap at atmospheric pressure. The resulting current pulse in each gap will be a triangle of about 20 ns basewidth carrying a charge of $\frac{1}{2} \times 380 \times 5 = 950$ electrons. The factor $\frac{1}{2}$ originates from the triangular shape of the signal. The configuration adopted to extract the signal from the chamber consists of the parallel combination of $n = 10$ branches, each made of $m = 6$ gaps in series. To evaluate the signal-to-noise ratio corresponding to a single pp interaction it will be assumed that the weighting function of the analog channel is piecewise parabolic. The corresponding shaper coefficients [8] are $A_1=1.33$ and $A_3=0.39$, in the physical case of unilateral noise spectra. The transistors employed in the preamplifier have a $\beta=120$. The value of the ballistic deficiency σ^2 is about 0.2. η_{opt} would be about 3. Therefore the system as it is meets the requirement of a charge measurement on the single bunch crossing and its signal-to-noise ratio is suitable for detecting a single pp interaction at LHC. However, as this type of detection system may be extended to other applications, it is interesting to discuss the measures to be taken in order to further improve the signal-to-noise ratio. They are basically two. One consists in operating the chamber at higher pressure which would result in an increased Q_{gap} . The second one in acting upon the mixture of gas to reduce the carrier collection time which would reduce the ballistic deficiency.

V. CONCLUSIONS

The detection system described in this paper consists of a multigap ionization chamber designed to stand extremely high radiation doses associated with an analog signal processor designed to perform charge measurements at a repetition rate of 40 MHz. The processor has been optimized to provide signal-to-noise ratio suitable to detect single pp interactions occurring in the LHC bunch crossing. The system was proven to suit the goal of measuring beam luminosity on a bunch by bunch basis.

APPENDIX

Consider the case of an ionization chamber, consisting of $n \times m$ equal gaps, where m and n are two integers, crossed by one MIP. Neglecting the Landau fluctuations, the charge induced in each gap by the carriers made available by the incoming particle, Q_{gap} , is the same for all the gap. It is assumed here that the signal from the chamber is a delta impulse of charge Q . The hypothesis will be made that the analog processor which acts on the chamber signal has a signal-to-noise ratio η_s^2 expressed as:

$$\eta_s^2 = \zeta \cdot \frac{Q^2}{C_D} \quad (6)$$

where ζ is the constant already defined in section II. It will

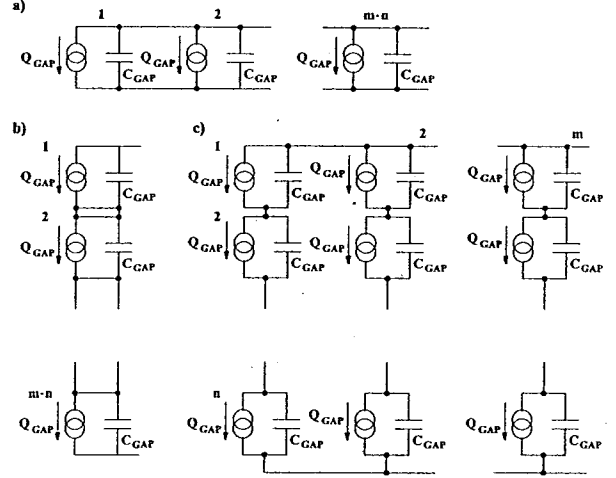


Fig. 6. Possible configurations of the $n \times m$ gaps: a) parallel connection; b) series connection; c) parallel connection of m branches, each consisting of the series combination of n gaps.

be demonstrated here that η_s^2 expressed by (6) is independent of the configuration in which the gaps are arranged. In other words, if the $n \times m$ gaps are connected in series or in parallel or if they are arranged in the parallel combination of m branches, each consisting of n gaps in series, η will be the same (see figure 6). To demonstrate this statement, consider first the case of the $n \times m$ gaps connected in series, in which $Q = Q_{gap}$ and $C_D = \frac{C_{gap}}{mn}$. The resulting η^2 according to (6) is

$$\eta_s^2 = \zeta \cdot \frac{mn \cdot Q_{gap}^2}{C_{gap}} \quad (7)$$

In the case of $n \times m$ gaps in parallel, $Q = nm \cdot Q_{gap}$ and $C_D = mnC_{gap}$, so that η^2 has the same form as in equation (7). Finally, in the case of the parallel combination of m branches, each consisting of n gaps in series, $Q = m \cdot Q_{gap}$ and $C_D = \frac{m}{n} \cdot C_{gap}$ which yields for η^2 the same value as for the previous cases. The following situations lead to equation (6).

1. Preamplifier featuring only series noise, sum of the channel thermal noise, with power spectral density S_0 , and $1/f$ noise, with power coefficient A_f . This is the typical case of a MOSFET preamplifier:

$$\eta_s^2 = \frac{Q^2}{C_D \left(\mu + \frac{1}{\mu} \right)^2 \left[H_0 \cdot \frac{A_1}{A_f} + H_f A_2 \right]} \quad (8)$$

In equation (8) $\mu = \sqrt{\frac{C_D}{C_i}}$ is the square root of the mismatch factor, $H_0 = S_0 C_i$, $H_f = A_f C_i$, A_1 has the same meaning as in equation (1) and A_2 is the shaper coefficient for $1/f$ noise.

2. Preamplifier featuring series white noise with power spectral density S_0 and parallel white noise with power spectral density S_p followed by a shaper, whose peaking

time t_p is set to its optimum value. In this case (concerning JFET and bipolar amplifiers)

$$\eta_s^2 = \frac{Q^2}{(C_D + C_i)^2 \cdot \frac{A_1}{t_p} \cdot S_0 + S_p A_3 t_p} \quad (9)$$

where A_1 and A_3 have the same meaning as in equation (1). The value of t_p at which η^2 attains its maximum is:

$$t_p = \sqrt{\frac{A_1}{A_3} \cdot (C_D + C_i) \cdot \frac{S_0}{S_p}} \quad (10)$$

and

$$\eta_{s,opt}^2 = \frac{Q^2}{2(C_D + C_i) \cdot \sqrt{A_1 A_3 S_0 S_p}} \quad (11)$$

As usually the size of the input device is such that $C_i = \alpha \cdot C_D$, where $\alpha \leq 1$, η^2 assumes the form

$$\eta_{s,opt}^2 = \frac{Q^2}{2C_D(1 + \alpha) \sqrt{A_1 A_3 S_0 S_p}} \quad (12)$$

3. Preamplifier with a bipolar transistor at the input. This is a particular case of the previous one and, neglecting C_i , optimum signal-to-noise ratio is

$$\eta_{s,opt}^2 = \frac{Q^2}{4kTC_D \cdot \sqrt{\frac{A_1 A_3}{\beta}}} \quad (13)$$

REFERENCES

- [1] W.C. Turner, "Instrumentation for the Absorbers in the Low Beta Insertions of LHC", LBNL-42180 (13 August 1998).
- [2] W.C. Turner, P.S. Datte, P.F. Manfredi, J.E. Millaud, N.V. Mokhov, M. Placidi et al., "Status Report on the Development of Instrumentation for Bunch by Bunch Measurement and Optimization of Luminosity in the LHC", *Proc. of US LHC Collaboration Meeting on Accelerator Physics Experiments for Future Hadron Colliders*, Brookhaven, 22-23 Feb. 2000.
- [3] W.C. Turner, E.H. Hoyer and N. Mokhov, "Absorbers for the High Luminosity Insertions of the LHC", *Proc. of EPAC 98*, Stockholm, 1998, p. 368.
- [4] W.C. Turner, M.T. Burks, P.S. Datte, P.F. Manfredi, J.E. Millaud, N.V. Mokhov et al., "Development of a detector for bunch by bunch measurement and optimization of luminosity in the LHC", *Nucl. Instr. and Meth. in Phys. Res. A*, Vol. 461 (1-3) (2001), pp. 107-110.
- [5] J.F. Beche, M.T. Burks, P.S. Datte, M. Haguenauer, P.F. Manfredi, J.E. Millaud et al., "An Ionization Chamber Shower Detector for the LHC Luminosity Monitor", due to appear on *IEEE Trans. Nucl. Sci.*, 2001.
- [6] E. Gatti, P.F. Manfredi, "Signal coupling from a semiconductor detector to a cold resistance preamplifier through a cable or a delay-line transformer", *IEEE Trans. Nucl. Sci.*, Vol. NS-25, No. 1, pp. 66-74, February 1978.
- [7] E. Gatti, A. Hrisoho, P.F. Manfredi, "Choice between FETs or bipolar transistor and optimization of their working points on low noise preamplifiers for fast pulse processing. Theory and experimental results", *IEEE Trans. Nucl. Sci.*, Vol. NS-30, No. 1, pp. 319-323, February 1983.
- [8] E. Gatti, P.F. Manfredi, M. Sampietro, V. Speziali, "Suboptimal filtering of 1/f-noise in detector charge measurement", *Nucl. Instr. and Meth. in Phys. Res. A*, Vol. 297 (1990), pp. 467-478.